Minkowski Interval Analysis for Tolerance Analysis in Linear Arrays

L. Tenuti, N. Anselmi, P. Rocca, M. Salucci, and A. Massa

Abstract

This work deals with the analysis of the effects of tolerances of the amplitude and phase weights on the radiation pattern of linear antenna arrays. A method based on the Minkowski Interval Analysis (M-IA) is exploited to analytically determine upper and lower bounds of the power pattern as a function of the maximum deviations of the control point values from the nominal values. In this document, after providing a mathematical description of the developed approach, some numerical results are reported to assess the effectiveness of the M-IA tool, as well as to compare it to a standard Cartesian IA-based (C-IA) approach, this latter being expected to provide larger (i.e., less reliable) bounds.

1 Variable Definition

This section is devoted at defining all the quantities will be find in the report.

1.1 Interval Analysis

- **Real Interval Numbers (Intervals)**

  A closed real interval $\mathbf{X} = [a,\, b]$, namely interval number $\mathbf{X}$, consists of the set of real numbers x such that $\{x : a \leq x \leq b\}$, i.e. it is the set of real numbers between and including the endpoints a and b. Consequently a real number x is equivalent to an interval $[x,\, x]$. Such an interval is said to be *degenerate* interval. A superscript L (or R) denotes the left (or right) endpoint of an interval. Thus if $\mathbf{X} = [a,\, b]$ then $\inf\{\mathbf{X}\} = a$ and $\sup\{\mathbf{X}\} = b$. Consequently, the right endpoint of the interval $\mathbf{X}$ is usually denoted as $\sup\{\mathbf{X}\}$ and the left endpoint of the interval is usually denoted as $\inf\{\mathbf{X}\}$.

  An interval $\mathbf{X} = [a, b]$ is said to be *positive* (or *non-negative*) if $a \geq 0$, *strictly positive* if $a > 0$, *negative* (or *non-positive*) if $b \leq 0$, and *strictly negative* if $b < 0$. Two intervals $[a, b]$ and $[c, d]$ are *equal* if and only if $a = c$ and $b = d$. Intervals are partially ordered. $[a, b] < [c, d] \Leftrightarrow b < c$.

- **Interval Arithmetic**

  Let us denote $+$, $-$, $*$ and $/$ the operation of addition, subtraction, multiplication and division, respectively. Let be *op* any one of these operations for the arithmetic of real numbers x and y, then the corresponding operation for the arithmetic of interval numbers $\mathbf{X}$ and $\mathbf{Y}$ is:

$$\mathbf{X}\, op\, \mathbf{Y} = \{x\, op\, y \,:\, x \in \mathbf{X},\, y \in \mathbf{Y}\}\,. \tag{1}$$

  From definition (1) follows that the interval $\mathbf{X}\, op\, \mathbf{Y}$ contains every possible number which can be formed as $x\, op\, y$ for each $x \in \mathbf{X}$ and $y \in \mathbf{Y}$. Moreover, following such a definition it is possible to produce the rules for generating the endpoints of $\mathbf{X}\, op\, \mathbf{Y}$ from the two interval operands $\mathbf{X}$ and $\mathbf{Y}$.

- **Interval Sum**

  Let be $\mathbf{X} = [\inf\{\mathbf{X}\}, \sup\{\mathbf{X}\}]$ and $\mathbf{Y} = [\inf\{\mathbf{Y}\}, \sup\{\mathbf{Y}\}]$ two real intervals. The sum operation is defined as:

$$\mathbf{X} + \mathbf{Y} = [\inf\{\mathbf{X}\} + \inf\{\mathbf{Y}\}, \sup\{\mathbf{X}\} + \sup\{\mathbf{Y}\}] \tag{2}$$

- **Interval Subtraction**

  Let be $\mathbf{X} = [\inf\{\mathbf{X}\}, \sup\{\mathbf{X}\}]$ and $\mathbf{Y} = [\inf\{\mathbf{Y}\}, \sup\{\mathbf{Y}\}]$ two real intervals. The subtraction operation is defined as:

$$\mathbf{X} - \mathbf{Y} = [\inf\{\mathbf{X}\} - \inf\{\mathbf{Y}\}, \sup\{\mathbf{X}\} - \sup\{\mathbf{Y}\}] \tag{3}$$

- **Interval Multiplication**

  Let be $\mathbf{X} = [\inf\{\mathbf{X}\}, \sup\{\mathbf{X}\}]$ and $\mathbf{Y} = [\inf\{\mathbf{Y}\}, \sup\{\mathbf{Y}\}]$ two real intervals. The multiplication operation is defined as:

$$\begin{aligned}\mathbf{X} * \mathbf{Y} \quad = \quad & [\min(\inf\{\mathbf{X}\}\inf\{\mathbf{Y}\}, \inf\{\mathbf{X}\}\inf\{\mathbf{Y}\}, \mathbf{X}_{\sup}\inf\{\mathbf{Y}\}, \sup\{\mathbf{X}\}\sup\{\mathbf{Y}\}), \\ & \max(\inf\{\mathbf{X}\}\inf\{\mathbf{Y}\}, \inf\{\mathbf{X}\}\sup\{\mathbf{Y}\}, \mathbf{X}_{\sup}\inf\{\mathbf{Y}\}, \sup\{\mathbf{X}\}\sup\{\mathbf{Y}\})]\end{aligned} \tag{4}$$

- **Interval Inverse**

  Let be$\mathbf{Y} = [\inf\{\mathbf{Y}\}, \sup\{\mathbf{Y}\}]$ a real interval. The inverse interval $1/\mathbf{Y}$ is defined as:

$$\frac{1}{\mathbf{Y}} = \left[\frac{1}{\sup\{\mathbf{Y}\}}, \frac{1}{\inf\{\mathbf{Y}\}}\right] \; 0 \notin \mathbf{Y} \tag{5}$$

- **Interval Division**

  Let be $\mathbf{X} = [\inf\{\mathbf{X}\}, \sup\{\mathbf{X}\}]$ and $\mathbf{Y} = [\inf\{\mathbf{Y}\}, \sup\{\mathbf{Y}\}]$ two real intervals. The interval division is defined by means of interval inverse and interval multiplication as:

$$\frac{\mathbf{X}}{\mathbf{Y}} = \mathbf{X} * \left(\frac{1}{\mathbf{Y}}\right) \; 0 \notin \mathbf{Y} \tag{6}$$

- **Power of a Real Interval**

  Let be $\mathbf{X} = [\inf\{\mathbf{X}\}, \sup\{\mathbf{X}\}]$ a real interval. The power of $\mathbf{X}$, $\mathbf{X}^n$ is a real interval computed as:

$$\mathbf{X}^n = \begin{cases} [1, 1] & if\, n = 0 \\ [\inf\{\mathbf{X}^n\}, \sup\{\mathbf{X}^n\}] & if\, \inf\{\mathbf{X}\} \geq 0 \, or \, if\, \inf\{\mathbf{X}\} \leq 0 \leq \sup\{\mathbf{X}\} \; and\, n\, is\, odd \\ [\sup\{\mathbf{X}^n\}, \inf\{\mathbf{X}^n\}] & if\, \sup\{\mathbf{X}\} \leq 0 \\ [0, \max(\inf\{\mathbf{X}^n\}, \sup\{\mathbf{X}^n\})] & if\, \inf\{\mathbf{X}\} \leq 0 \leq \sup\{\mathbf{X}\} \; and\, n\, is\, even \end{cases} \tag{7}$$

- **Square of a Real Interval**

  Let be $\mathbf{X} = [\inf\{\mathbf{X}\}, \sup\{\mathbf{X}\}]$ a real interval. Accordingly to equation (7) the square of the interval $\mathbf{X}$, $\mathbf{X}^2$ is an interval computed as:

$$\mathbf{X}^2 = \begin{cases} [\inf\{\mathbf{X}^2\}, \sup\{\mathbf{X}^2\}] & if\, \inf\{\mathbf{X}\} \geq 0 \\ [\sup\{\mathbf{X}^2\}, \inf\{\mathbf{X}^2\}] & if\, \sup\{\mathbf{X}\} \leq 0 \\ [0, \max(\inf\{\mathbf{X}^n\}, \sup\{\mathbf{X}^n\})] & if\, \inf\{\mathbf{X}\} \leq 0 \leq \sup\{\mathbf{X}\} \end{cases} \tag{8}$$

- **Width of a Real Interval**

  Let be $\mathbf{X} = [\inf\{\mathbf{X}\}, \sup\{\mathbf{X}\}]$ a real interval. The width of the interval $\mathbf{X}$, $w(\mathbf{X})$ is a real number defined as:

$$w(\mathbf{X}) = \sup\{\mathbf{X}\} - \inf\{\mathbf{X}\} \tag{9}$$

- **Center of a Real Interval - Middle point**

  Let be $\mathbf{X} = [\inf\{\mathbf{X}\}, \sup\{\mathbf{X}\}]$ a real interval. The middle point of the interval $\mathbf{X}$, $m(\mathbf{X})$ is defined as:

$$m(\mathbf{X}) = \frac{\sup\{\mathbf{X}\} + \inf\{\mathbf{X}\}}{2} \tag{10}$$

- **Equivalent representation of Intervals**

  Let be $\mathbf{X} = [\inf\{\mathbf{X}\}, \sup\{\mathbf{X}\}]$ a real interval, it can be represent equivalently in the form:

$$\mathbf{X} = \left[m(\mathbf{X}) - \frac{w(\mathbf{X})}{2}; m(\mathbf{X}) + \frac{w(\mathbf{X})}{2}\right] \tag{11}$$

- **Absolute value of a Real Interval**

  Let be $\mathbf{X} = [\inf\{\mathbf{X}\}, \sup\{\mathbf{X}\}]$ a real interval, the absolute value of an interval is:

$$|\mathbf{X}| = \max(|\inf\{\mathbf{X}\}|, |\sup\{\mathbf{X}\}|) \tag{12}$$

- **Complex Interval Numbers (Intervals)**

  A complex intervals $\mathbf{C}$ is an ordered pair of intervals $\mathbf{C} = [\mathbf{X}, \mathbf{Y}]$ with $\mathbf{X} = [\inf\{\mathbf{X}\}, \sup\{\mathbf{X}\}]$ and $\mathbf{X} = [\inf\{\mathbf{Y}\}, \sup\{\mathbf{Y}\}]$real intervals. It consists in the set of complex numbers $x + iy$ such that:

$$\mathbf{X} = \{x + iy \ \inf\{\mathbf{X}\} \leq x \leq \sup\{\mathbf{X}\} \ \inf\{\mathbf{Y}\} \leq y \leq \sup\{\mathbf{Y}\}\} \tag{13}$$

- **Negative of a Complex Interval**

  Let be $\mathbf{C} = [\mathbf{X}, \mathbf{Y}]$ with $\mathbf{X} = [\inf\{\mathbf{X}\}, \sup\{\mathbf{X}\}]$ and $\mathbf{Y} = [\inf\{\mathbf{Y}\}, \sup\{\mathbf{Y}\}]$real intervals. The negative of $\mathbf{C}$, $-\mathbf{C}$ is defined as:

$$-\mathbf{C} = [-\mathbf{X}, -\mathbf{Y}] \tag{14}$$

  where in equation (14), $-\mathbf{X}$ is the real interval $-\mathbf{X} = [-\sup\{\mathbf{X}\}, -\inf\{\mathbf{X}\}]$ and $-\mathbf{Y}$ is the real interval $-\mathbf{Y} = [-\sup\{\mathbf{Y}\}, -\inf\{\mathbf{Y}\}]$.

- **Complex Conjugate Complex Interval**

  Let be $\mathbf{C} = [\mathbf{X}, \mathbf{Y}]$ with $\mathbf{X} = [\inf\{\mathbf{X}\}, \sup\{\mathbf{X}\}]$ and $\mathbf{X} = [\inf\{\mathbf{Y}\}, \sup\{\mathbf{Y}\}]$real intervals. The complex conjugate of the complex interval $\mathbf{C}$, $\mathbf{C}*$ is defined as:

$$\mathbf{C}^* = [\mathbf{X}, -\mathbf{Y}] \tag{15}$$

- **Sum of Complex Intervals (Cartesian Sum)**

  Let be $\mathbf{C} = [\mathbf{X},\, \mathbf{Y}]$ and $\mathbf{C}' = [\mathbf{X}',\, \mathbf{Y}']$ two complex intervals. The sum of the complex intervals is a complex interval defined as:

$$\mathbf{C} + \mathbf{C}' = [\mathbf{X} + \mathbf{X}',\, \mathbf{Y} + \mathbf{Y}'] \tag{16}$$

- **Product of Complex Intervals**

  Let be $\mathbf{C} = [\mathbf{X},\, \mathbf{Y}]$ and $\mathbf{C}' = [\mathbf{X}',\, \mathbf{Y}']$ two complex intervals. The product of the complex intervals is a complex interval defined as:

$$\mathbf{C} \cdot \mathbf{C}' = [\mathbf{X}\mathbf{X}' - \mathbf{Y}\mathbf{Y}',\, \mathbf{X}\mathbf{Y}' + \mathbf{Y}\mathbf{X}'] \tag{17}$$

- **Sum of a complex interval and its complex conjugate**

  Let be $\mathbf{C} = [\mathbf{X},\, \mathbf{Y}]$ a complex interval and $\mathbf{C}* = [\mathbf{X},\, -\mathbf{Y}]$ its complex conjugate. The sum $\mathbf{C}$ and $\mathbf{C}*$ is the real interval defined as:

$$\mathbf{X} + \mathbf{X}^* = [2\mathbf{X}] \tag{18}$$

- **Product of a complex interval and its complex conjugate**

  Let be $\mathbf{C} = [\mathbf{X},\, \mathbf{Y}]$ a complex interval and $\mathbf{C}* = [\mathbf{X},\, -\mathbf{Y}]$ its complex conjugate. The product of $\mathbf{C}$ and its complex conjugate $\mathbf{C}*$ is the real interval:

$$\mathbf{X} \cdot \mathbf{X}* = \left[\mathbf{X^2} + \mathbf{Y^2}\right] \tag{19}$$

- **Absolute value of a Complex Interval**

  Let be $\mathbf{C} = [\mathbf{X},\, \mathbf{Y}]$ a complex interval, the absolute value of the interval $\mathbf{C}$ is:

$$|\mathbf{C}| = \sup\left\{\mathbf{X^2} + \mathbf{Y^2}\right\} \tag{20}$$

1.2 Complex Interval in Polar form (Interval Phasors)

- **Polar complex Interval**

  Let be $[\rho] \subset \mathbb{R}^+$ and $[\theta] \subset \mathbb{R}^+$. The set defined by $Z = \left\{z \in \mathbb{C} : z = \rho \exp^{j\theta};\, \rho \in [\rho], \theta \in [\theta]\right\}$ is called polar complex interval. A polar interval can be uniquely characterized by two real intervals: $[\rho] = [\inf\{[\rho]\}, \sup\{[\rho]\}]$ and $[\theta] = [\inf\{[\theta]\}, \sup\{[\theta]\}]$.

- **Sum of polar complex intervals**

  Let be $[Z_1] = [\rho_1] \exp^{j[\theta_1]}$ and $[Z_2] = [\rho_2] \exp^{j[\theta_2]}$ two complex intervals expressed in polar notation. The interval magnitude and the interval phase of the interval sum $[Z_s] = [\rho_s] \exp^{j[\theta_s]}$ are computed solving the following minimization /maximization problems. The magnitude of every element of $[Z_s]$ can be computed using:

$$|z_s| = \left|\rho_1 \exp^{j\theta_1} + \rho_2 \exp^{j\theta_2}\right| = \sqrt{\rho_1^2 + \rho_2^2 + 2\rho_1\rho_2 \cos(\theta_1 - \theta_2)} \tag{21}$$

being $\rho_1 \in [\rho_1]$, $\rho_2 \in [\rho_2]$, $\theta_1 \in [\theta_1]$ and $\theta_2 \in [\theta_2]$. Then, the bounds of $[\rho_s] = [\inf([\rho_s]), \sup([\rho_s])]$ must verify:

$$\begin{aligned} \inf([\rho_s]) &= \min_{\rho_s \in Z_1 \oplus Z_2} |z_s| \\ \sup([\rho_s]) &= \max_{\rho_s \in Z_1 \oplus Z_2} |z_s| \end{aligned} \tag{22}$$

with $Z_1 \oplus Z_2 = \{z_1 + z_2 \,|\, z_1 \in [Z_1], z_2 \in [Z_2]\}$ call as Minkowski Sum. On the other hand, the phase of every elements of $[Z_s]$ can be computed as:

$$\theta_s = \arctan \frac{\rho_1 \sin\theta_1 + \rho_2 \sin\theta_2}{\rho_1 \cos\theta_1 + \rho_2 \cos\theta_2} \tag{23}$$

with $\rho_1 \in [\rho_1]$, $\rho_2 \in [\rho_2]$, $\theta_1 \in [\theta_1]$ and $\theta_2 \in [\theta_2]$. The bounds for the interval phase $[\theta_s] = [\inf(\theta_s), \sup(\theta_s)]$ are solutions of:

$$\begin{aligned} \inf([\theta_s]) &= \min_{\rho_s \in Z_1 \oplus Z_2} \theta_s \\ \sup([\theta_s]) &= \max_{\rho_s \in Z_1 \oplus Z_2} \theta_s \end{aligned} \tag{24}$$

Properties and Observations:

1. Commutative. $[Z_1] + [Z_2] = [Z_2] + [Z_1]$
2. Not associative. $[Z_1] + [Z_2] + [Z_3] = ([Z_1] + [Z_2]) + [Z_3] \neq [Z_1] + ([Z_2] + [Z_3])$
3. The sum of two polar intervals can produce wide interval bounds .

1.3 Convex Sets and Minkowski sum

- **Convex set and Convex Hull:**

  A subset S of the plane is called *convex* if and only if for any pair of points $\underline{p}$ and $\underline{q} \in S$, the line segment $\underline{p}\,\underline{q}$ is completely contained in S. The *convex hull* $CH\,(S)$ of the set S is the smallest convex set that contains S.

- **Minkowski sum:**

  Let be $S_1 \subset \mathbb{R}^2$ and $S_2 \subset \mathbb{R}^2$ two sets of vectors in R^2. The Minkowski sum of S_1 and S_2, denoted as $S_1 \oplus S_2$ is defined as:

$$S_1 \oplus S_2 = \{\underline{s}_1 + \underline{s}_2 \,:\, \underline{s}_1 \in S_1\, \underline{s}_2 \in S_2\} \tag{25}$$

  where, $\underline{s}_1 + \underline{s}_2$ denotes the vectorial sum of the vector $\underline{s}_1$ and $\underline{s}_2$, that is , if $\underline{s}_1 = (s_{1x},\, s_{1y})$ and $\underline{s}_2 = (s_{2x},\, s_{2y})$, $\underline{s}_1 + \underline{s}_2 = (s_{1x} + s_{1y},\, s_{2x} + s_{2y})$. Let us observe that the definition of the Minkowski sum is equivalent to the definition of Interval Sum for complex intervals (2) and (16).

  Properties:

  1. Associative. $S_1 \oplus S_2 \oplus S_3 = (S_1 \oplus S_2) \oplus S_3 = S_1 \oplus (S_2 \oplus S_3)$
  2. Distributive. $S_1 \oplus S_2 = S_1 \oplus (S_{2,1} \oplus S_{2,2})$ with $S_{2,1} \oplus S_{2,2} = S_2$
  3. Commutative: $S_1 \oplus S_2 = S_2 \oplus S_1$.
  4. The Minkowski sum of two convex sets is a convex set.

  Computational Costs

  Let be P and R two polygons with N and M vertices, respectively. The complexity of the Minkowski sum $P \oplus R$ is bounded as follows:

  - $O\,(N + M)$ if both the polygons are convex;
  - $O\,(NM)$ if one polygon is convex and one is non-convex;
  - $O\left(N^2 M^2\right)$ if both the polygons are non-convex;

1.4 Array Analysis

- **Array Factor - Linear Array:**

  The array factor of an uniform linear array is defined as:

$$AF\left(\theta\right) = \sum_{n=1}^{N} w_n e^{j(n-1)k \cdot d \sin(\theta)} \, \theta \in \left[-\frac{\pi}{2}; \frac{\pi}{2}\right] \tag{26}$$

  where $w_n \in \mathbb{C}$; $n = 1, \dots, N$ are the control points of the N elements of the array, is the element spacing, θ is the angle measured from the array axis.

- Array Factor - Planar Array:

The array factor of a uniform planar array is defined as:

$$AF\left(\theta, \phi\right) = \sum_{n=1}^{N}$$

- **Array Excitations:**

$$w_n = \alpha_n \cdot e^{j\beta_n} \tag{27}$$

  where α_n; $n = 1, \dots, N$ are the amplitudes and β_n; $n = 1, \dots, N$ are the phases of the w_n; $n = 1, \dots, N$ excitation coefficients.

- **Variable u:**

$$u = \sin\theta \, \theta \in \left[-\frac{\pi}{2}; \frac{\pi}{2}\right] \tag{28}$$

- **Normalized Array Factor:**

$$AF\left(\theta\right)_n = \frac{AF\left(\theta\right)}{\max_\theta \left\{\left|AF\left(\theta\right)\right|\right\}} \, \theta \in \left[-\frac{\pi}{2}; \frac{\pi}{2}\right] \tag{29}$$

  where in (29) $\max_\theta \left\{\left|AF\left(\theta\right)\right|\right\}$ is the maximal value of $\left|AF\left(\theta\right)\right|$ $\theta \in \left[-\frac{\pi}{2}; \frac{\pi}{2}\right]$.

- **Position of the maximum of AF:**

$$u_{\max} = u \in [-1; 1] \; AF(u_{\max}) = \max\left\{AF\left(u\right)\right\} \, u \in [-1; 1] \tag{30}$$

- **Power Pattern:**

  The power pattern radiated by an antenna array is computed as follows:

$$P\left(\theta\right) = AF\left(\theta\right) AF\left(\theta\right)^* = \left|AF\left(\theta\right)\right|^2 = Re^2\left\{AF\left(\theta\right)\right\} + Im^2\left\{AF\left(\theta\right)\right\} \tag{31}$$

where in equation (31) $AF(\theta)^*$ is the complex-conjugate of the $AF(\theta)$.

- $3\,[dB]$ **Beam Width** $HPBW$**:**

$$HPBW = \theta_A - \theta_B \tag{32}$$

where $\theta_A$and θ_B are the angular positions where $|AF(\theta)|_n^2 = -3\,[dB]$

- **Normalized Power Level** P_{RL}**:**

$$P_{RL}(\theta) = 20 \cdot \log_{10} |AF(\theta)|_n \tag{33}$$

- **First Null Position** ψ_1**:**

Position of the first null of $|AF(\theta)|_n$

- **Maximal** SLL $\max\{SLL\}$**:**

It is the maximal level of the grating lobes of $|AF(\theta)|_n$.

- **Maximal** *Directivity* - D_{max}**:**

The directivity is defined as:

$$D(\theta, \phi) = \frac{U(\theta, \phi)}{\frac{1}{4\pi}\int_0^{\pi}\int_0^{2\pi} U(\theta, \phi)\sin(\theta)\, d\theta d\phi} \tag{34}$$

where $U(\theta, \phi)$ is the radiation intensity:

$$U(\theta, \phi) = \frac{r^2}{2\eta}\left|\underline{E}_{tot}(\underline{r}, \theta, \phi)\right|^2 = U_0(\theta, \phi)\, |AF(\theta, \phi)|^2 \tag{35}$$

$U_0(\theta, \phi)$ is radiation intensity for the single element. In our case, considering ideal isotropic sources, $U_0(\theta, \phi) = 1$. Usually "peak directivity" is more used, that is the directivity calculated at its maximum: $D_{max}(\theta_0, \phi_0)$. For our array, the direction of the maximum is at $\theta = 0$; thus :

$$U(\theta_0, \phi_0) = |AF(\theta_0, \phi_0)|^2 = \left|\sum_{n=1}^{N} w_n e^{j(n-1)k\cdot d\cdot \sin(\theta_0)}\right|^2 = \left|\sum_{n=1}^{N} a_n\right|^2 \tag{36}$$

Now, computing the denominator of (34), we obtain:

$$\frac{1}{4\pi}\int_0^{\pi}\int_0^{2\pi} U(\theta, \phi) sin(\theta) d\theta d\phi = \sum_{n=1}^{N}\sum_{m=1}^{N} w_n w_m^* \int_{-1}^{1} e^{jkd(n-m)u} du \tag{37}$$

which for $d = \frac{\lambda}{2}$ reduces to $\left|\sum_{n=0}^{N-1} w_n\right|^2$, obtaining the expression of peak directivity:

$$D_{max} = \frac{\left|\sum_{n=1}^{N} w_n\right|^2}{\sum_{n=0}^{N-1} |w_n|^2} \tag{38}$$

valid for half-wavelength-spaced isotropic elements.

1.5 Interval Array Analysis

- **Interval Control Point - $\mathbf{W}_n$**; $n = 1, \dots, N$

The interval control points of a linear array of N elements are defined as:

$$\mathbf{W}_n = \mathbf{A}_n \exp^{j\mathbf{B}_n};\ n = 1, \dots, N \tag{39}$$

where in equation (39) $\mathbf{A}_n = [\inf\{\mathbf{A}_n\}; \sup\{\mathbf{A}_n\}]$, $n = 1, \dots, N$ are the interval control point amplitudes being:

$$\inf\{\mathbf{A}_n\} = \alpha_n - \varepsilon_n^{(inf)};\ n = 1, \dots, N \tag{40}$$

$$\sup\{\mathbf{A}_n\} = \alpha_n + \varepsilon_n^{(sup)};\ n = 1, \dots, N \tag{41}$$

with α_n; $n = 1, \dots, N$ the reference value of the $n-th$ control point amplitude, and $\varepsilon_n^{(inf)}$; $n = 1, \dots, N$, $\varepsilon_n^{(sup)}$; $n = 1, \dots, N$ the lower and upper amplitude tolerance on the n-th control point, respectively. On the other hand, $\mathbf{B}_n = [\inf\{\mathbf{B}_n\}; \sup\{\mathbf{B}_n\}]$, $n = 1, \dots, N$ are the interval control point phases being:

$$\inf\{\mathbf{B}_n\} = \beta_n - \delta_n^{(inf)};\ n = 1, \dots, N \tag{42}$$

$$\sup\{\mathbf{B}_n\} = \beta_n + \delta_n^{(sup)};\ n = 1, \dots, N \tag{43}$$

with β_n; $n = 1, \dots, N$ the reference value of the $n-th$ control point phase, $\delta_n^{(inf)}$; $n = 1, \dots, N$, $\delta_n^{(sup)}$; $n = 1, \dots, N$ the lower and upper phase tolerance for the n-th control point, respectively.

- **Interval Array Factor AF**

Let us define the Interval Array Factor **AF** of an uniformly spaced linear array as follows:

$$\mathbf{AF}(\theta) = \sum_{n=1}^{N} \mathbf{W}_n e^{j\Theta_n} \tag{44}$$

where $j = \sqrt{-1}$ is the complex variable and $\Theta_n = (kd(n-1)\sin\theta)$; $n = 1, \dots, N$, being $k = \frac{2\pi}{\lambda}$ the free-space wavenumber and λ the wavelength, d the inter-element spacing and $\theta \in \left[-\frac{\pi}{2}; \frac{\pi}{2}\right]$ the angular direction measured from boresight. Substituting (39) in (44) we obtain:

$$\mathbf{AF}(\theta) = \sum_{n=1}^{N} \mathbf{A}_n e^{j(\Theta_n + \mathbf{B}_n)} \tag{45}$$

- **Interval Power Pattern P**

The interval power pattern $\mathbf{P}$ is a real interval computed by means of the following equation:

$$\mathbf{P}(\theta) = \Re^2\{\mathbf{AF}(\theta)\} + \Im^2\{\mathbf{AF}(\theta)\} \tag{46}$$

being $\Re\{\mathbf{AF}(\theta)\}$, $\Im\{\mathbf{AF}(\theta)\}$ two real intervals bounding the real and the imaginary part of the array factor, respectively. Alternatively, the interval power pattern can be compute as:

$$\mathbf{P}(\theta) = |\mathbf{AF}(\theta)|^2 \tag{47}$$

being $|\mathbf{AF}(\theta)|$ a real interval bounding the magnitude of the vectors included in the complex interval $\mathbf{AF}(\theta)$.

- **Interval Directivity D**

Using expression (38), we can compute the interval directivity $\mathbf{D}$ as follows:

$$\mathbf{D}_{\max} = \frac{\left|\sum_{n=1}^{N} \mathbf{W}_n\right|^2}{\sum_{n=1}^{N} \mathbf{W}_n^2} \tag{48}$$

- **Side Lobe Level for Interval Arrays**

It's important to define a proper interval version for the significant figure of merit SLL. In our case we can derive from the interval radiation pattern, two different beam patterns:

$$\inf\{\mathbf{P}(u)\} = \inf\left\{|AF(u)|^2\right\} \tag{49}$$

$$\sup\{\mathbf{P}(u)\} = \sup\left\{|AF(u)|^2\right\} \tag{50}$$

Now let us define the interval SLL as $\mathbf{SLL} = [\inf\{SLL\}, \sup\{SLL\}]$ where:

$$\inf\{SLL\} = -\left[\max_{u \in ML}\{\inf\{\mathbf{P}(u)\}\} - \max_{u \in SL}\{\inf\{\mathbf{P}(u)\}\}\right] \tag{51}$$

$$\sup\{SLL\} = -\left[\max_{u \in ML}\{\inf\{\mathbf{P}(u)\}\} - \max_{u \in SL}\{\sup\{\mathbf{P}(u)\}\}\right] \tag{52}$$

where ML and SL are the sets of u corresponding to the Main Lobe and the Side Lobes regions.

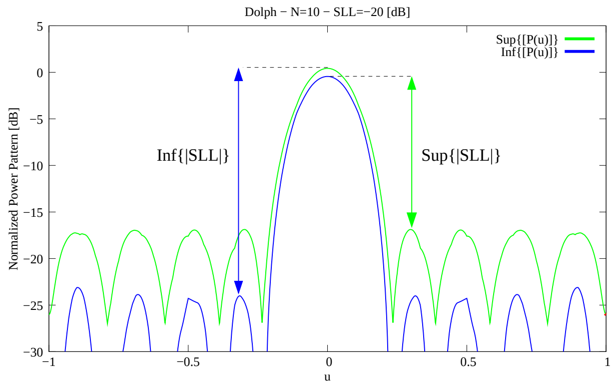

Figure: **SLL**

- **Half Power Beam Width - 3dB**

  Let us the interval HPBW, as $\mathbf{BW} = [\inf\{\mathbf{BW}\}, \sup\{\mathbf{BW}\}]$ where $\inf\{\mathbf{BW}\}$ and $\sup\{\mathbf{BW}\}$ are described by in the following figure:

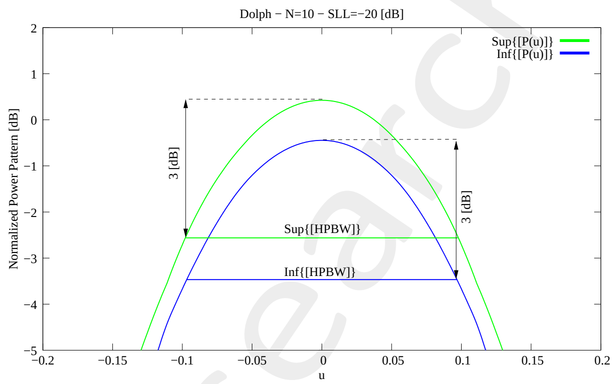

Figure: Infimum and Supremum of **BW** - 3dB

- **Pattern Tolerance**

  The Pattern Tolerance parameter $\triangle$ measures the area between the $\sup\{\mathbf{P}(u)\}$ and $\inf\{\mathbf{P}(u)\}$ and it is defined as:

$$\triangle = \int_{-1}^{1} \left(\sup\{\mathbf{P}(u)\} - \inf\{\mathbf{P}(u)\}\right) du \tag{53}$$

  A graphical representation of the pattern matching is shown in the following figure.

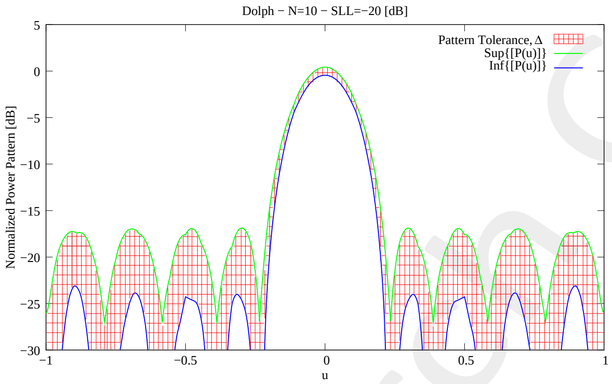

Figure: Pattern Tolerance

- **Normalized Pattern Tolerance**

  The Normalized Pattern Tolerance parameter $\triangle_n$ measures the area between the the $\sup\{\mathbf{P}(u)\}$ and $\inf\{\mathbf{P}(u)\}$ divided by the radiated power $P(u)$.

$$\Delta_n = \frac{\int_{-1}^{1} \left(\sup\{\mathbf{P}(u)\} - \inf\{\mathbf{P}(u)\}\right) du}{\int_{-1}^{1} P(u)\, du} \tag{54}$$

- **Peak Interval**

  This parameter measure the gap between the infimum and the supremum radiation patterns at the peak of them.

$$\mathbf{P}_{\max} = \left[\inf\{\mathbf{P}_{\max}\}, \sup\{\mathbf{P}_{\max}\}\right] \tag{55}$$

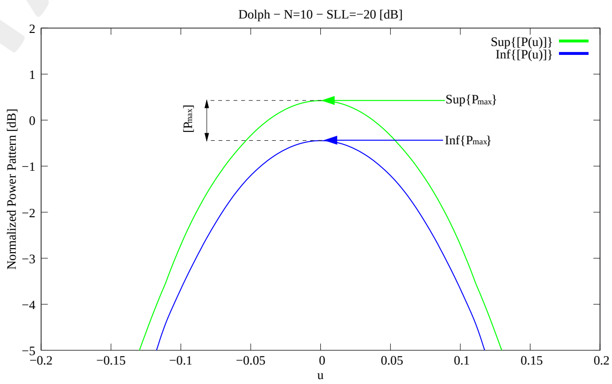

Figure: Peak Interval Parameter

1.6 Computation of the Interval Array Factor

Let us consider the computation of the interval array factor **AF** as described by equation (45) here reported for sake of clearness:

$$\mathbf{AF}(\theta) = \sum_{n=1}^{N} \mathbf{A}_n e^{j(\Theta_n + \mathbf{B}_n)} \tag{56}$$

It turns out that the **AF** is the sum of N polar intervals (interval phasors). In order to compute (56) we can use using different strategies, using different interval representations for the interval control points $\mathbf{W}_n$; $n = 1, \ldots, N$. In the following we consider three possible choice: the Cartesian sum, the polar sum and the Minkowski sum of convex set with particular emphasis on the latter.

1.6.1 Cartesian sum

The computation of the interval far-field pattern can be performed using the Cartesian representation. More in detail, let us express the interval control points $\mathbf{W}_n = \mathbf{A}_n \exp^{j\mathbf{B}_n}$; $n = 1, \ldots, N$ in Cartesian notation as:

$$\mathbf{W}_n = \mathbf{A}_n \exp^{j\mathbf{B}_n} = [\mathbf{A}_n \cos \mathbf{B}_n,\, \mathbf{A}_n \sin \mathbf{B}_n]\,;\; n = 1, \ldots, N \tag{57}$$

where $\mathbf{A}_n \cos \mathbf{B}_n = \Re\{\mathbf{W}_n\}$ and $\mathbf{A}_n \sin \mathbf{B}_n = \Im\{\mathbf{W}_n\}$; $n = 1, \ldots, N$ are the real and the imaginary part of the interval control point. Unfortunately, using this representation the interval phasor is bounded by a complex rectangular set that overestimates the dimensions of the interval phasor as clearly shown in Figure 1. This redundancy in bounding the interval phasor produces not precise bounds when considering the interval sum operation.

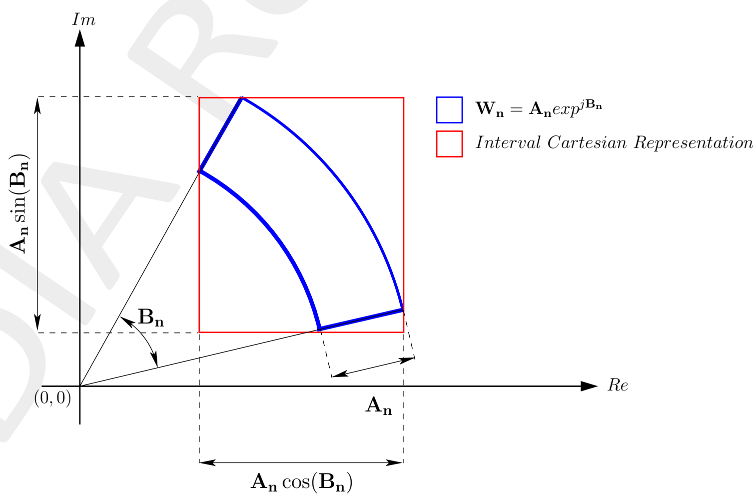

Figure 1

On the other hand the **AF** can be easily and quickly computed as:

$$\Re\{\mathbf{AF}\} = \sum_{n=1}^{N} \mathbf{A}_n \cos(\mathbf{B}_n + \Theta_n) \tag{58}$$

$$\Im\{\mathbf{AF}\} = \sum_{n=1}^{N} \mathbf{A}_n \sin(\mathbf{B}_n + \Theta_n) \tag{59}$$

and the interval power pattern $\mathbf{P}(\theta)$ is:

$$\mathbf{P}(\theta) = \Re^2\{\mathbf{AF}(\theta)\} + \Im^2\{\mathbf{AF}(\theta)\} = |\mathbf{AF}(\theta)|^2$$

1.6.2 Polar Sum

The **AF** can be computed representing the interval phasors using the interval polar form, following the algorithm reported in 1.2. Even if it could seem that the use of the polar sum leads to sharpest bounds with respect to the Cartesian representation this is not generally true. The main reason seems to be related with the fact that the sum of two interval is not a polar interval. As a consequence, the polar sum leads to sharpest bounds with respect to the interval sum just when adding two phasors. As a consequence, the polar sum cannot be used when dealing with **AF** computation, since it consider the sum of $N > 2$ terms.

1.6.3 Minkowski sum

Following the observations reported in the previous sections now we are looking for a strategy able to perform the sum of interval complex phasors quickly and with minimal bounds. A possible solution considers the use of the Minkowski sum of convex sets. The use of convex sets with respect to non-convex sets is justified by the fact that the algorithm for computing the Minkowski sum of convex sets is faster with respect to the sum of non-convex sets. The algorithm for computing the **AF** can be summarized by the following steps:

1. Determine the smaller convex set S_n including the interval phasor terms of the array factor $\mathbf{A}_n e^{j(\Theta_n+\mathbf{B}_n)}$, $n = 1, \ldots, N$ (Convex Hull);
2. Add the convex sets using the Minkowski sum;
3. Compute the Infimum and the Supremum value of the magnitude of the Minkowski sum, $\inf\{|\mathbf{AF}(\theta)|\}$ and $\sup\{|\mathbf{AF}(\theta)|\}$;
4. Compute the interval power pattern $\mathbf{P}(\theta) = \left[\inf\{|\mathbf{AF}|\}^2, \sup\{|\mathbf{AF}|\}^2\right]$.

Minimal Convex Sets - Convex Hull of Interval Phasors

Let us consider an interval phasors, $[Z] = [\rho]\exp^{j[\theta]}$ identified by the interval magnitude $[\rho] = [\inf\{[\rho]\}, \sup\{[\rho]\}]$ and interval phase $[\theta] = [\inf\{[\theta]\}, \sup\{[\theta]\}]$. From the definition of convex set follows that the convex hull of the interval phasor, $S_Z \subset \mathbb{C}$ is the set defined by:

- The segment between the points:
  - $A = (\inf\{[\rho]\}\cos(\inf\{[\theta]\}), \inf\{[\rho]\}\sin(\inf\{[\theta]\}))$ and

- $B = (\sup\{[\rho]\}\cos(\inf\{[\theta]\}), \sup\{[\rho]\}\sin(\inf\{[\theta]\}))$;

- The arc between the points:
  - $B = (\sup\{[\rho]\}\cos(\inf\{[\theta]\}), \sup\{[\rho]\}\sin(\inf\{[\theta]\}))$ and
  - $C = (\sup\{[\rho]\}\cos(\sup\{[\theta]\}), \sup\{[\rho]\}\sin(\sup\{[\theta]\}))$;

- The segment between the points:
  - $C = (\sup\{[\rho]\}\cos(\inf\{[\theta]\}), \sup\{[\rho]\}\sin(\inf\{[\theta]\}))$ and
  - $D = (\inf\{[\rho]\}\cos(\sup\{[\theta]\}), \inf\{[\rho]\}\sin(\sup\{[\theta]\}))$;

- The segment between the points:
  - $D = (\inf\{[\rho]\}\cos(\sup\{[\theta]\}), \inf\{[\rho]\}\sin(\sup\{[\theta]\}))$ and
  - $A = (\inf\{[\rho]\}\cos(\inf\{[\theta]\}), \inf\{[\rho]\}\sin(\inf\{[\theta]\}))$.

A pictorial representation of the convex hull of an interval phasor is shown in Figure 2.

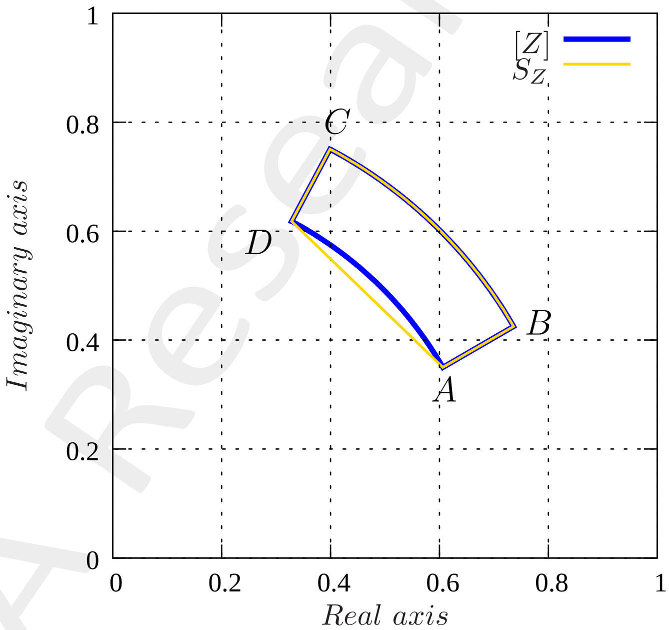

Figure 2

Since the arc between the points A and B contains infinite points, the computation cost for the Minkowski sum will be infinite. In order to overcome such a drawback let us approximate the circular arc with a regular polygon P of L sides that inscribes the circle of radius $\sup\{[\rho]\}$. From geometrical considerations the vertices of the regular polygon will lie on the circumference of radius R:

$$R = \frac{\sup\{[\rho]\}}{\cos\left(\frac{\pi}{L}\right)} \tag{60}$$

If we choose L sufficiently big (e.g., if $L = 360$ $R = 1.0004 \sup\{[\rho]\}$) a good approximation of the arc can be obtained. The vertices of the regular polygon P will have the following coordinates: $P = \left\{(x_p,\, y_p)\,;\, x_p = R\cos\left(\frac{2\pi}{L}p\right)\,;\, y_p = R\sin\right.$ Accordingly the “approximated” convex set including the interval phasor $[Z]$ will be defined by the following points:

- The segment between the points:
  - $A = (\inf\{[\rho]\}\cos(\inf\{[\theta]\})\,,\, \inf\{[\rho]\}\sin(\inf\{[\theta]\}))$ and
  - $B = (\sup\{[\rho]\}\cos(\inf\{[\theta]\})\,,\, \sup\{[\rho]\}\sin(\inf\{[\theta]\}))$;
- The broken line defined by the vertices of the polygon P with phase included in the interval $[\theta]$:
  - $P* = \left\{(x_p,\, y_p)\,;\, x_p = R\cos\left(\frac{2\pi}{L}p\right)\,;\, y_p = R\sin\left(\frac{2\pi}{L}p\right)\,;\, p = 0, \ldots, L-1\right\}$ with $\inf\{[\theta]\} < \frac{2\pi}{L}p < \sup\{[\theta]\}$;
- The segment between the points:
  - $C = (\sup\{[\rho]\}\cos(\inf\{[\theta]\})\,,\, \sup\{[\rho]\}\sin(\inf\{[\theta]\}))$ and
  - $D = (\inf\{[\rho]\}\cos(\sup\{[\theta]\})\,,\, \inf\{[\rho]\}\sin(\sup\{[\theta]\}))$;
- The segment between the points:
  - $D = (\inf\{[\rho]\}\cos(\sup\{[\theta]\})\,,\, \inf\{[\rho]\}\sin(\sup\{[\theta]\}))$ and
  - $A = (\inf\{[\rho]\}\cos(\inf\{[\theta]\})\,,\, \inf\{[\rho]\}\sin(\inf\{[\theta]\}))$.

In defining the convex set, we have considered the duality between $\mathbb{R}^2$ and the complex plane $\mathbb{C}$. Accordingly, the point $z = (x,\, y)$ in $\mathbb{R}^2$ means the complex value $z = x + iy$ in $\mathbb{C}$. For sake of comparison between the bounds obtained by means of convex set and with complex Cartesian intervals are shown in Figure 3.

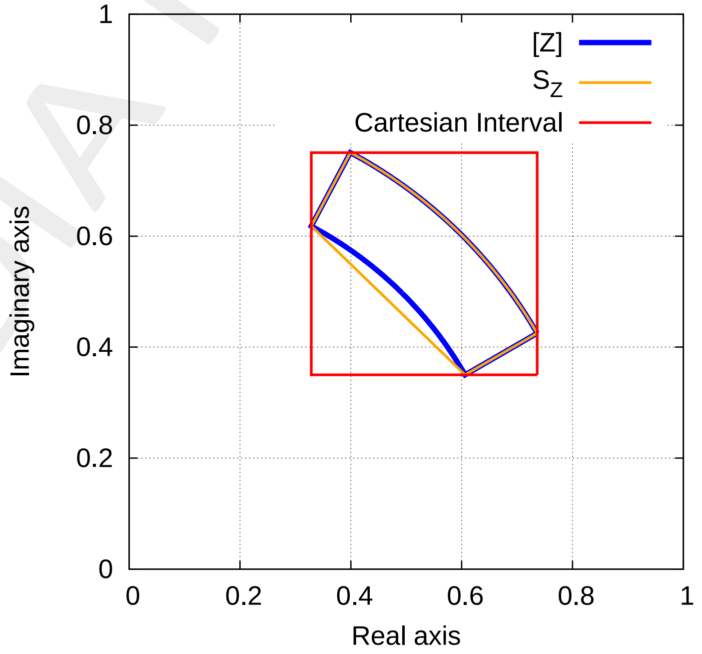

Figure 3

The convex set perform a better inclusion with respect to the complex Cartesian interval. As a matter of fact there is just a small overestimation of the polar interval in the convex set due by the segment between the points $(\sup\{[\rho]\}\cos(\inf\{[\theta]\}), \sup\{[\rho]\}\sin(\inf\{[\theta]\}))$ and $(\inf\{[\rho]\}\cos(\sup\{[\theta]\}), \inf\{[\rho]\}\sin(\sup\{[\theta]\}))$.

Minkowski Sum Algorithm

Once the complex interval phasors have been bounded by properly defined convex sets, the sum of all the convex sets can be computed efficiently observing that any vertex of the Minkowski sum is the the sum of two original vertices that are extreme in a common direction. Accordingly, the Minkowski sum of two convex sets can be computed using the algorithm described by the following pseudo-code:

`Algorithm MINKOWSKI SUM (S,T)`

`Input:`

`Convex set` S `with` N `vertices` $\underline{s}_1, \dots, \underline{s}_N$

`Convex set` T `with` M `vertices` $\underline{t}_1, \dots, \underline{t}_M$.

`The list of the vertices are assumed to be in counter-clockwise order,`

`with` $\underline{s}_1$ `and` $\underline{t}_1$ `the vertices with smallest` y`-coordinate.`

`Output:`

`Minkowski sum,` $S \oplus T$.

1. INITIALIZATION

$n \leftarrow 1$, $m \leftarrow 1$

$\underline{s}_{N+1} \leftarrow \underline{s}_1$, $\underline{s}_{N+2} \leftarrow \underline{s}_2$, $\underline{t}_{M+1} \leftarrow \underline{t}_1$, $\underline{t}_{M+2} \leftarrow \underline{t}_2$

2. MINKOWSKI SUM COMPUTATION

`repeat`

    `Add` $\underline{s}_n + \underline{t}_m$ `as vertex of` $S \oplus T$

    `if` $angle(\underline{s}_n \underline{s}_{n+1}) < angle(\underline{t}_m \underline{t}_{m+1})$ `then`

        $n \leftarrow n+1$

    `else if` $angle(\underline{s}_n \underline{s}_{n+1}) > angle(\underline{t}_m \underline{t}_{m+1})$ `then`

        $m \leftarrow m+1$

    `else`

        $n \leftarrow n+1$

        $m \leftarrow m+1$

`until` $n = N+1$ `and` $m = M+1$

where in the algorithm the notation $angle\left(\underline{s}_n \underline{s}_{n+1}\right)$ indicate the angle that the vector $\underline{t}_n \underline{t}_{n+1}$ makes with the positive x-axis. Applying iteratively the algorithm it is possible to compute the values of $\mathbf{AF}(\theta)$, that it turns out to be a convex set, defined by H vertices $\mathbf{AF}(\theta) = \{(x_h, y_h); h = 1, \dots, H\}$.

Infimum and Supremum of $|\mathbf{AF}(\theta)|$

The infimum and the supremum value of the magnitude of the elements belonging to the interval $\mathbf{AF}(\theta)$ can be computed as the minimal (maximal) value of a radius of a circumference centered in the origin, ρ such that one point of the circumference belongs to $\mathbf{AF}(\theta)$. Mathematically, this can be expressed as:

$$\inf\{|\mathbf{AF}(\theta)|\} = \min\left\{\rho : \rho^2 \in \mathbf{AF}(\theta)\right\} \tag{61}$$

$$\sup\left\{\left|\mathbf{AF}\left(\theta\right)\right|\right\} = \max\left\{\rho\,:\,\rho^2 \in \mathbf{AF}\left(\theta\right)\right\} \tag{62}$$

For sake of clearness a pictorial representation of the infimum and supremum of a convex set is shown in Figure 4.

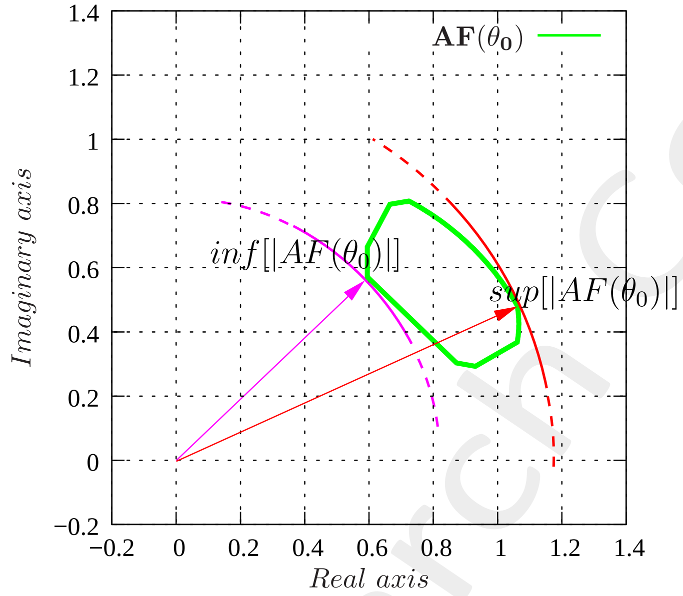

Figure 4

2 Numerical Assessment - Method Validation - Linear Array

GOAL: This section has two main objectives: prove that the bounds obtained using the Minkowski sum are smaller with respect to one obtained using the Cartesian sum, but they remain still inclusive. Moreover, the results will give some indications about the dimensions and the shape of the **AF** intervals.

Array geometry:

- Uniform linear array: $N = 10$.
- Inter-element spacing: $d = 0.5$ $[\lambda]$.

Nominal control points:

- Taylor pattern - $SLL = 20$ $[dB]$ - $\overline{n} = 2$.

Tolerances on the control points:

- Amplitude tolerance: $\delta\alpha_n = 0\%$, $\pm 1\,\%$.
- Phase tolerance: $\delta\beta_n = \pm 1$, ± 5 $[deg]$.

Minkowski sum parameters:

- Number of sides including polygon: $L = 720$

Number of Random Patterns: 10^4 trials

2.1 Amplitude Tolerance: $\delta\alpha_n = 0\,\%$ - Phase Tolerance: $\delta\beta_n = \pm 1,\, \pm 5\ [deg]$

Interval Excitations

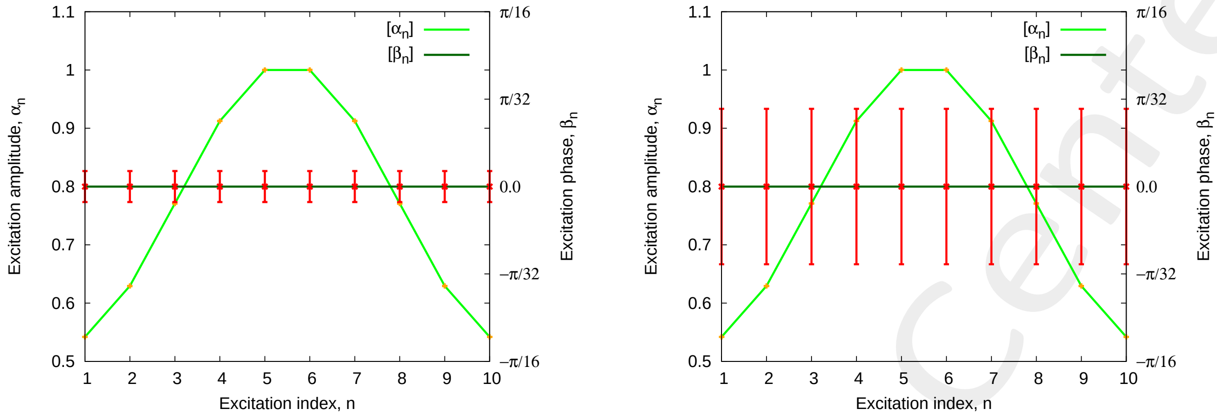

(a) (b)

Figure 5

Interval Patterns - $u \in [-1,\, 1]$

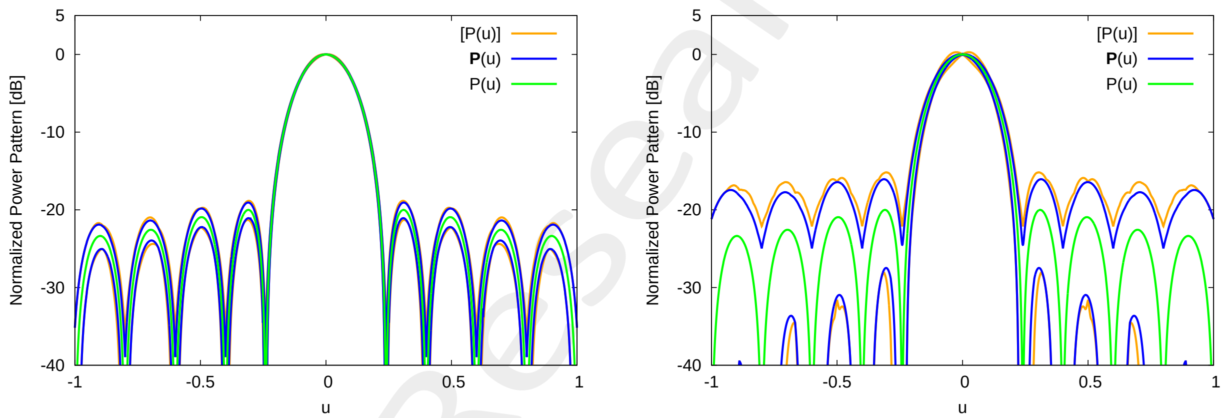

(a) (b)

Figure 6

Interval Patterns - Main Lobe Region

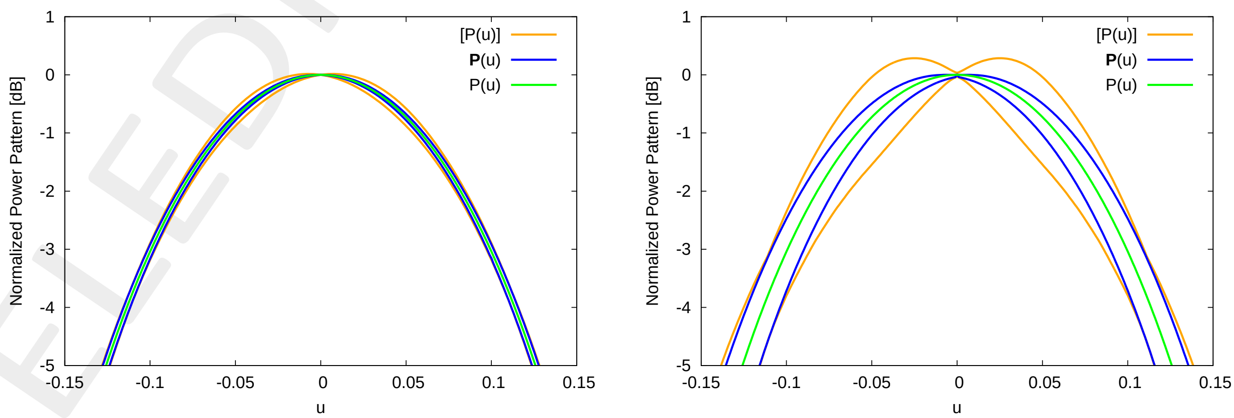

(a) (b)

Figure 7

Interval Array Factor samples

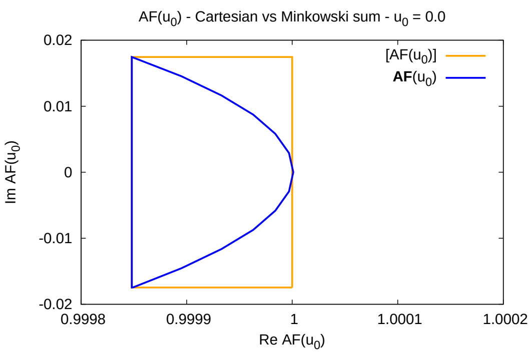

(a)

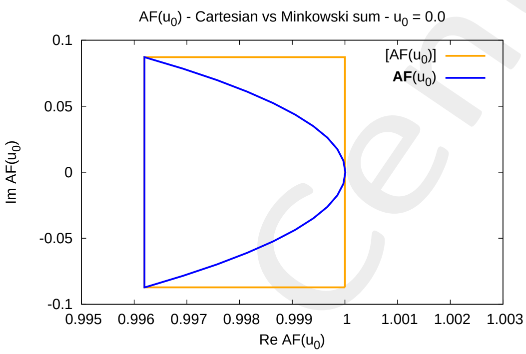

(b)

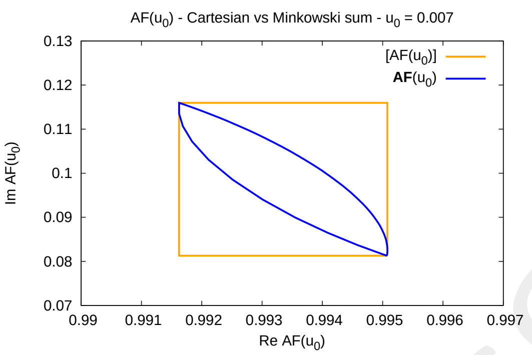

(c)

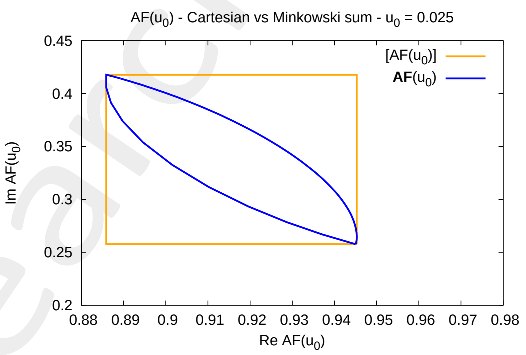

(d)

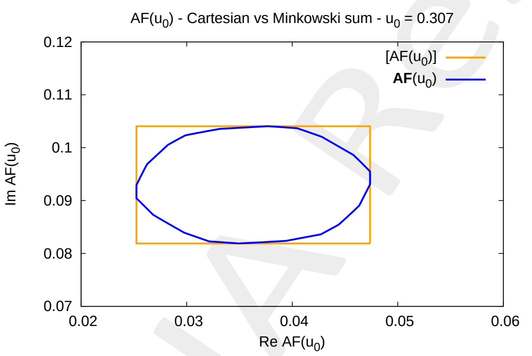

(e)

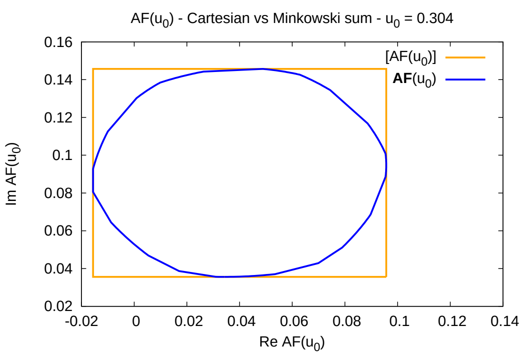

(f)

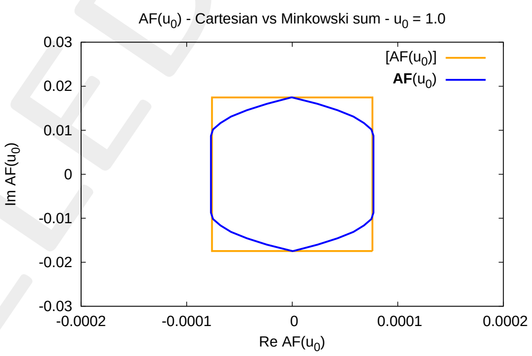

(g)

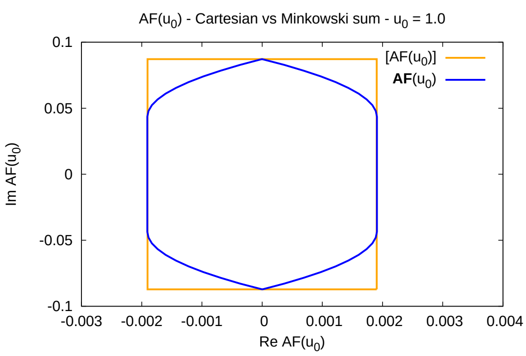

(h)

Figure 8

Interval Array Factor Samples - $\delta\alpha_n = 0\,\%$ - $\delta\beta_n = \pm 1$ $[deg]$

	$u_0 = 0.0$	$u_0 = 0.007$	$u_0 = 0.307$	$u_0 = 1.0$
$[\|AF(u_0)\|]$	[0.9998, 1.00015]	[0.995, 1.002]	[0.0857, 0.114]	[0.0, 0.0175]
$\|\mathbf{AF}(u_0)\|$	[0.9998, 1.00000]	[0.997, 0.999]	[0.0883, 0.111]	[0.0, 0.0174]

Table I

Interval Array Factor Samples - $\delta\alpha_n = 0\,\%$ - $\delta\beta_n = \pm 5$ $[deg]$

	$u_0 = 0.0$	$u_0 = 0.025$	$u_0 = 0.304$	$u_0 = 1.0$
$[\|AF(u_0)\|]$	[0.996, 1.004]	[0.922, 1.033]	[0.0356, 0.1742]	[0.0, 0.0872]
$\|\mathbf{AF}(u_0)\|$	[0.996, 1.000]	[0.961, 0.991]	[0.0422, 0.1558]	[0.0, 0.0871]

Table II

Interval Pattern Features

$Feature$	$Nominal$	$Cartesian\,Sum$		$Minkowski\,Sum$	
		$\delta\beta_n = \pm 1$ $[deg]$	$\delta\beta_n = \pm 5$ $[deg]$	$\delta\beta_n = \pm 1$ $[deg]$	$\delta\beta_n = \pm 5$ $[deg]$
BW $[u]$	0.200	[0.196, 0.204]	[0.186, 0.228]	[0.196, 0.204]	[0.180, 0.220]
SLL $[dB]$	-20.0	$[-21.30, -18.84]$	$[-28.38, -15.14]$	$[-21.07, -19.06]$	$[-27.48, -16.03]$
$P_{\max}$ $[dB]$	0.0	$[-0.00132, 0.0157]$	$[-0.033, 0.286]$	$[-0.00132, 0.0]$	$[-0.033, 0.0]$
Δ	–	0.0180	0.0929	0.0116	0.0589
Δ_{norm}	–	0.0513	0.2654	0.0331	0.1682

Table III

Comments and Observations:

The Minkowski interval are always included in the Cartesian interval. Accordingly, the related interval parameters are included in the Cartesian intervals, and the values of the pattern matching and the normalized pattern matching Δ and Δ_{norm} are smaller in the first case. As expected, the Cartesian interval has always a rectangular shape, whereas the Minkowski interval can assume different shapes, however it always remains convex. Moreover, the Cartesian interval perfectly includes the Minkowski set, and the maximal/minimal values for the Real/Imaginary part of the array factor are the same in both cases. What it is different is the magnitude of the array factor that is always smaller for the Minkowski set. The main difference between the Cartesian and the Minkowski bounds occurs in the side-lobe level region, but it is in the main beam that we can clearly understand the redundancy problem, since the supremum of the power pattern using Cartesian intervals assumes not physical values since a phase error cannot lead to a power amplification.

Interval Patterns vs Random Pattern $u \in [-1, 1]$

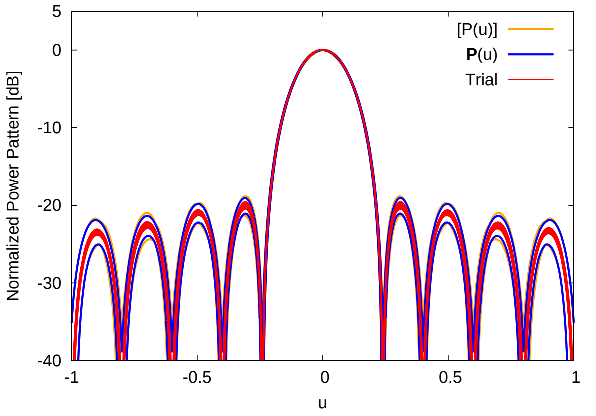

(a)

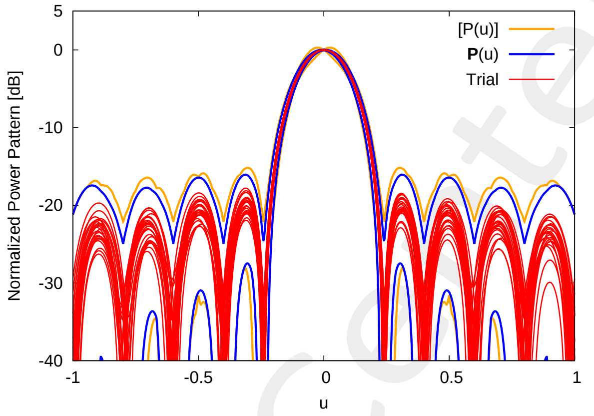

(b)

Figure 9

Interval Patterns vs Random Pattern - Main Lobe Region

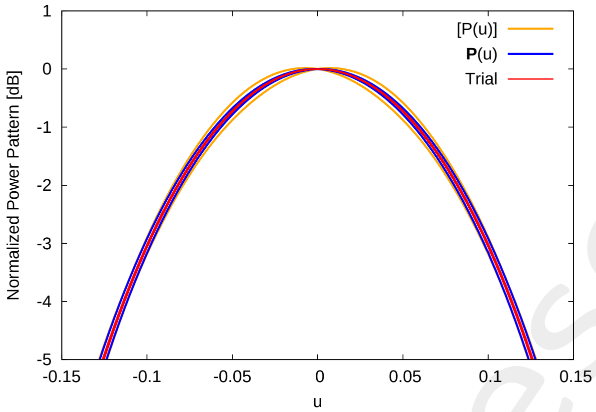

(a)

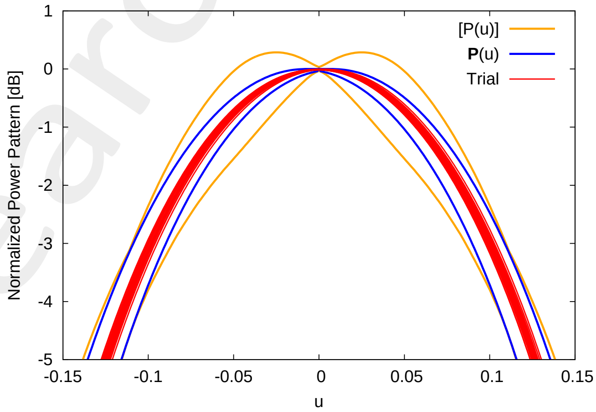

(b)

Figure 10

Interval Array Factor samples vs Random samples

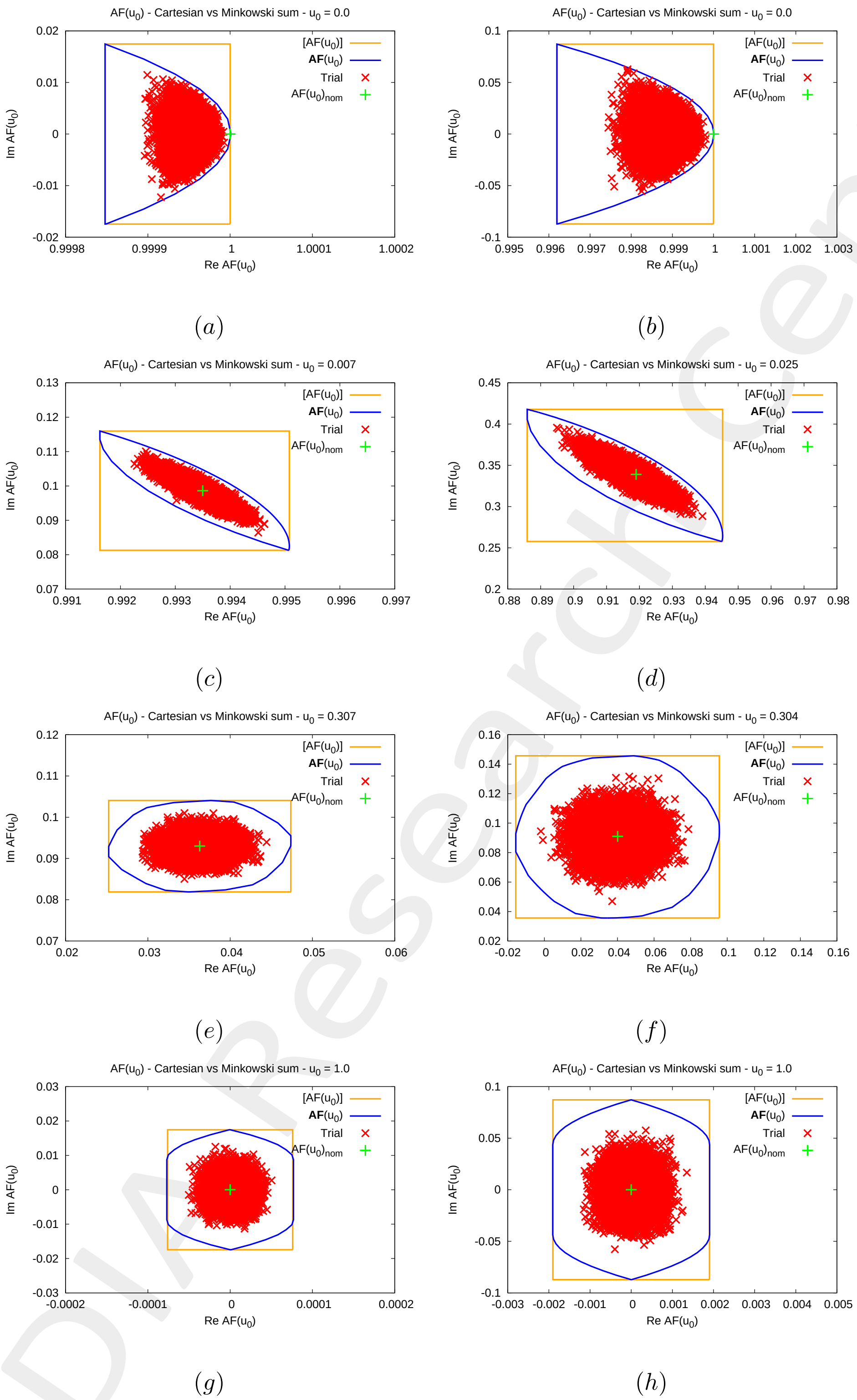

Figure 11

Interval Pattern Features vs Random Pattern Features

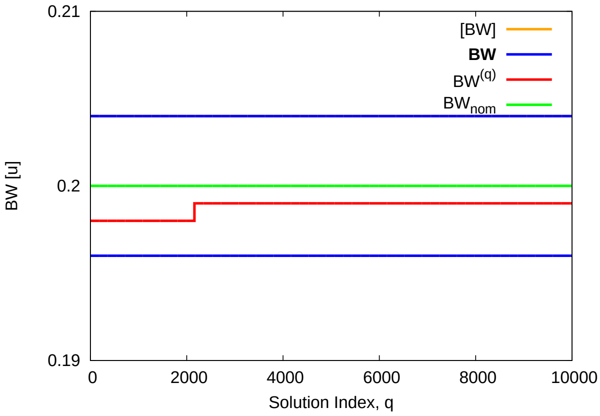

(*a*)

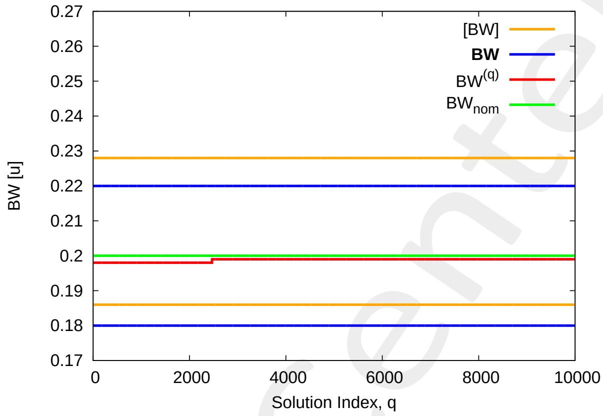

(*b*)

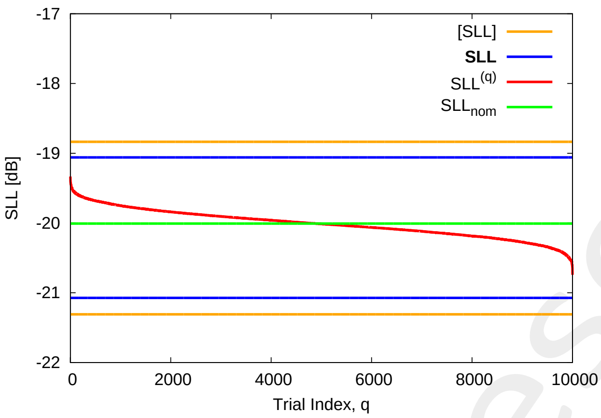

(*a*)

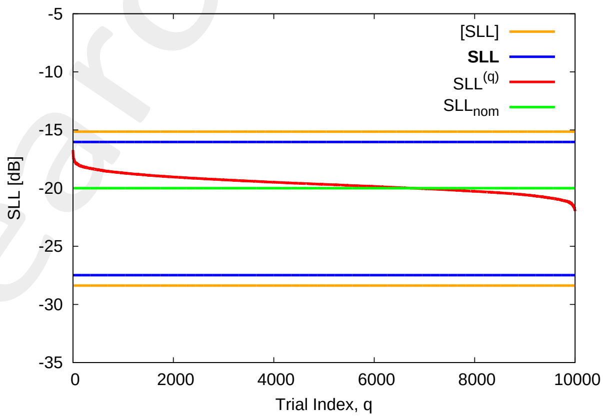

(*b*)

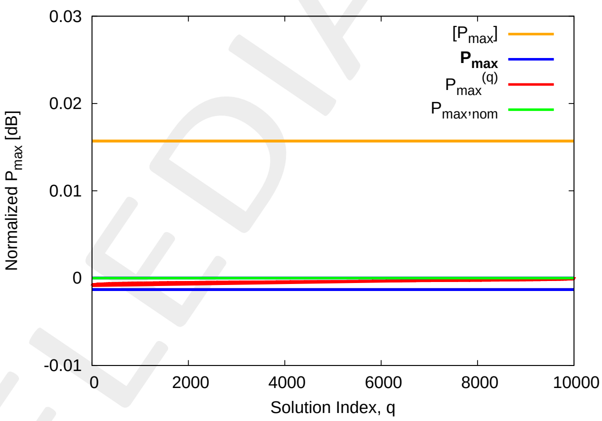

(*a*)

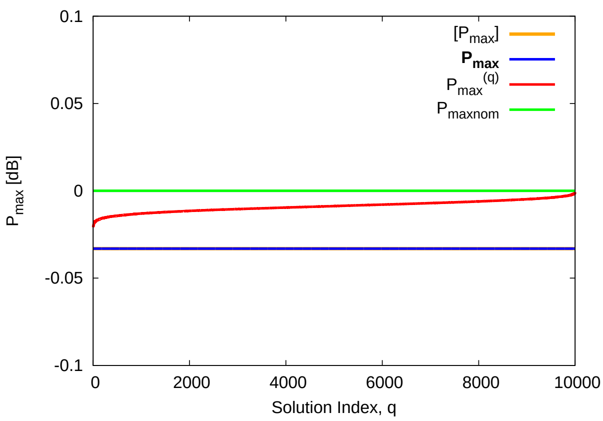

(*b*)

Figure 12

2.1.1 Comments and Observations:

Considering 10000 random patterns, the inclusivity for both Cartesian and Minkowski interval seems assured for small ± 1 $[deg]$ and big ± 5 $[deg]$ phase error. It is worth of noting that even if some redundancy occurs in both the intervals (Fig. 11), it seems very small for the Minkowski intervals. Moreover, the distance between the Supremum and Infimum of the interval Minkowski and Cartesian interval is not constant. Such a result can be explained considering that the redundancy phenomena is not constant with respect to the angular variable u.

References

[1] N. Anselmi, P. Rocca, M. Salucci, and A. Massa, "Optimization of excitation tolerances for robust beamforming in linear arrays," *IET Microw. Antennas Propag.*, vol. 10, no. 2, pp. 208-214, 2016.

[2] P. Rocca, G. Oliveri, R. J. Mailloux, and A. Massa, "Unconventional phased array architectures and design Methodologies - A review," *Proc. IEEE*, vol. 104, no. 3, pp. 544-560, Mar. 2016.

[3] G. Oliveri, M. Salucci, and A. Massa, "Synthesis of modular contiguously clustered linear arrays through a sparseness-regularized solver," *IEEE Trans. Antennas Propag,*, vol. 64, no. 10, pp. 4277-4287, Oct. 2016.

[4] L. Poli, P. Rocca, N. Anselmi, and A. Massa, "Dealing with uncertainties on phase weighting of linear antenna arrays by means of interval-based tolerance analysis," *IEEE Trans. Antennas Propag.*, vol. 63, no. 7, pp. 3299-3234, Jul. 2015.

[5] P. Rocca, N. Anselmi, and A. Massa, "Optimal synthesis of robust beamformer weights exploiting interval analysis and convex optimization," *IEEE Trans. Antennas Propag.*, vol. 62, no. 7, pp. 3603-3612, Jul. 2014.

[6] L. Manica, N. Anselmi, P. Rocca, and A. Massa, "Robust mask-constrained linear array synthesis through an interval-based particle swarm optimisation," *IET Microw. Antennas Propag.*, vol. 7, no. 12, pp. 976-984, Sep. 2013.

[7] N. Anselmi, L. Manica, P. Rocca, and A. Massa, "Tolerance analysis of antenna arrays through interval arithmetic," *IEEE Trans. Antennas Propag.*, vol. 61, no. 11, pp. 5496-5507, Nov. 2013.

[8] P. Rocca, L. Manica, N. Anselmi, and A. Massa, "Analysis of the pattern tolerances in linear arrays with arbitrary amplitude errors," *IEEE Antennas Wireless Propag. Lett.*, vol. 12, pp. 639-642, 2013.

[9] T. Moriyama, L. Poli, N. Anselmi, M. Salucci, and P. Rocca, "Real array pattern tolerances from amplitude excitation errors," *IEICE Electron. Express*, vol. 11, no. 17, pp. 1-8, Sep. 2014.

[10] P. Rocca, N. Anselmi, and A. Massa, "Optimal synthesis of robust array configurations exploiting interval analysis and convex optimization," *IEEE Trans. Antennas Propag.*, vol. 62, no. 7, pp. 3603-3612, Jul. 2014.

[11] N. Anselmi, P. Rocca, M. Salucci, and A. Massa, "Power pattern sensitivity to calibration errors and mutual coupling in linear arrays through circular interval arithmetics," *Sensors*, vol. 16, no. 6 (791), pp. 1-14, 2016.

[12] L. Tenuti, N. Anselmi, P. Rocca, M. Salucci, and A. Massa, "Minkowski sum method for planar arrays sensitivity analysis with uncertain-but-bounded excitation tolerances," *IEEE Trans. Antennas Propag.*, vol. 65, no. 1, pp. 167-177, Jan. 2017.

[13] P. Rocca, N. Anselmi, and A. Massa, "Interval Arithmetic for pattern tolerance analysis of parabolic reflectors," *IEEE Trans. Antennas Propag.*, vol. 62, no. 10, pp. 4952-4960, Oct. 2014.

[14] P. Rocca, L. Poli, N. Anselmi, M. Salucci, and A. Massa, "Predicting antenna pattern degradations in microstrip reflectarrays through interval arithmetic," *IET Microw. Antennas Propag.*, vol. 10, no. 8, pp. 817-826, May 2016.

[15] N. Anselmi, M. Salucci, P. Rocca, and A. Massa, "Generalized sensitivity analysis tool for pattern distortions in reflector antennas with bump-like surface deformations," *IET Microw. Antennas Propag.*, vol. 10, no. 9, p. 909-916, Jun. 2016.